

## Slow-Binding Human Serine Racemase Inhibitors from High-Throughput Screening of Combinatorial Libraries

Seth M. Dixon,<sup>†</sup> Pu Li,<sup>†</sup> Ruiwu Liu,<sup>‡</sup> Herman Wolosker,<sup>§</sup> Kit S. Lam,<sup>‡</sup> Mark J. Kurth,<sup>\*,†</sup> and Michael D. Toney<sup>\*,†</sup>

Department of Chemistry, University of California, One Shields Avenue, Davis, California 95616, Division of Hematology and Oncology, Department of Internal Medicine, UC Davis Cancer Center, University of California, Davis, 4501 X Street, Sacramento, California 95817, and Department of Biochemistry, The B. Rappaport Faculty of Medicine, Technion-Israel Institute of Technology, Haifa 31096, Israel

Received July 21, 2005

One-bead one-compound combinatorial chemistry together with a high-throughput screen based on fluorescently labeled enzyme allowed the identification of slow binding inhibitors of human serine racemase (hSR). A peptide library of topographically segregated encoded resin beads was synthesized, and several hSR-binding compounds were isolated, identified, and resynthesized for further kinetic study. Of these, several showed inhibitory effects with moderate potency (high micromolar  $K_{iS}$ ) toward hSR. A clear structural motif was identified consisting of 3-phenylpropionic acid and histidine moieties. Importantly, the inhibitors identified showed no structural similarities to the natural substrate, L-serine. Detailed kinetic analyses of the properties of selected inhibitors show that the screening protocol used here selectively identifies slow binding inhibitors. They provide a pharmacophore for the future isolation of more potent ligands that may prove useful in probing and understanding the biological role of hSR.

### Introduction

The D stereoisomers of amino acids were long believed to exist only in bacteria and invertebrates. This view has changed over the past decade with the discovery of D-serine and D-aspartate in the mammalian nervous system.<sup>1</sup> The pyridoxal phosphate (PLP)<sup>a</sup> enzyme serine racemase, which is enriched in astrocytes in mammalian brain, has been shown to be responsible for the physiological conversion of L-serine to D-serine, as well as  $\alpha/\beta$  elimination of water from both stereoisomers of serine.<sup>2, 3</sup>

D-Serine occurs at high levels in the mammalian brain, higher than even some common amino acids, and it has been shown to be an endogenous ligand for the “glycine site” of N-methyl-D-aspartate (NMDA) receptors (Figure 1).<sup>4–6</sup> These receptors play central roles in excitatory neurotransmission, neuronal plasticity, and learning and memory.<sup>7–10</sup> D-Serine may additionally mediate the light-dependent increase in neuronal activity of vertebrate retina by activating NMDA receptors.<sup>11</sup> It has also been suggested to be involved in long-term potentiation in the hippocampus, indicating a role for D-serine in synaptic plasticity.<sup>12</sup> Serine racemase and D-serine have also recently been found in the peripheral nervous system.<sup>13</sup>

Mammalian serine racemase has structural similarities with fold-type II PLP enzymes, such as the bacterial enzymes serine/threonine dehydratase and D-serine dehydratase.<sup>2,14</sup> The  $\alpha/\beta$  elimination activity of serine racemase therefore reflects its evolutionary origins. The initial rates of racemization and elimination of L-serine by serine racemase are strongly stimulated by magnesium and ATP, indicating that the Mg<sup>+</sup>ATP complex is a physiological ligand of the enzyme.<sup>15</sup>

Over activation of the NMDA receptor is proposed to be responsible for the cell death that occurs in strokes. In support of this proposal, blockers of the D-serine binding site of the NMDA receptor are neuroprotective in animal models of stroke.<sup>16</sup> Other studies suggest that D-serine and NMDA receptor dysfunction play a role in the pathophysiology of schizophrenia<sup>17,18</sup> and may play a role in the pathophysiology of Alzheimer's disease.<sup>19</sup> In the human placenta, serine racemase produces D-serine, which is then introduced into fetal blood.<sup>20</sup> The involvement of D-serine in this breadth of pathophysiological processes makes serine racemase an excellent drug target.

A variety of inhibitor discovery approaches are available to the experimentalist. These include the traditional synthesis of individual target compounds,<sup>21,22</sup> synthesis of small libraries of molecules using combinatorial methods,<sup>23,24</sup> and the screening of large combinatorial libraries.<sup>25–33</sup> Our approach with human serine racemase (hSR) involves the latter, employing the one-bead one-compound combinatorial approach that has proven to be an effective tool in biological research.<sup>34–36</sup>

One of our goals in this work was to develop a facile, adaptable, and robust method for large-scale on-bead screening of complex combinatorial libraries for serine racemase inhibitors. Several colorimetric<sup>37</sup> and fluorescence-based<sup>38–40</sup> assays for the identification of positive beads have been described in the literature. Herein, we describe the application of an enzyme (i.e., serine racemase) fluorescently labeled with commercially available, activated dyes in large-scale on-bead screening.<sup>41</sup> The labeled enzyme is incubated with the library, the beads are examined under a fluorescence microscope, and positive beads are picked and identified (Figure 2). Using this methodology, we have identified a series of peptide inhibitors of serine racemase that bear no structural relation to serine.

### Results

A model one-bead one-compound, encoded N-terminally capped peptide-based combinatorial library consisting of 74 088 compounds [42 Fmoc amino acids (2 $\times$ ) and 42 carboxylic acids; 42  $\times$  42  $\times$  42 = 74 088 compounds] was synthesized on Tentagel resin according to Scheme 1;<sup>42</sup> the diversity elements

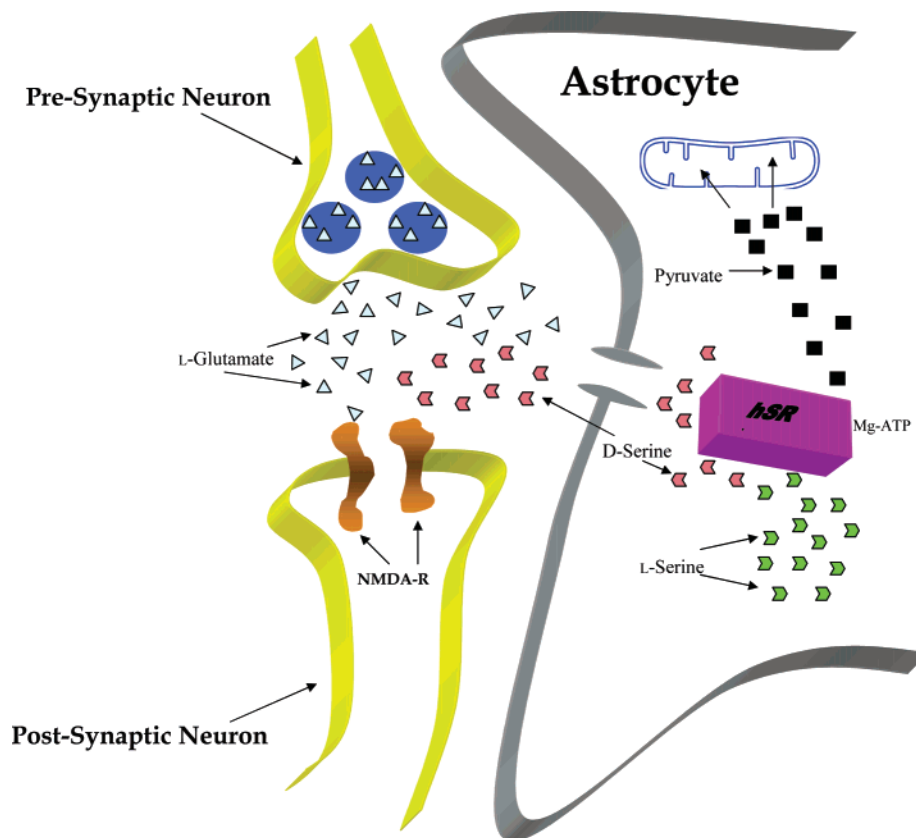
\* Corresponding authors. Fax: 530-752-8995; Email: mjkurth@ucdavis.edu or mdtoney@ucdavis.edu.

<sup>†</sup> Department of Chemistry, University of California.

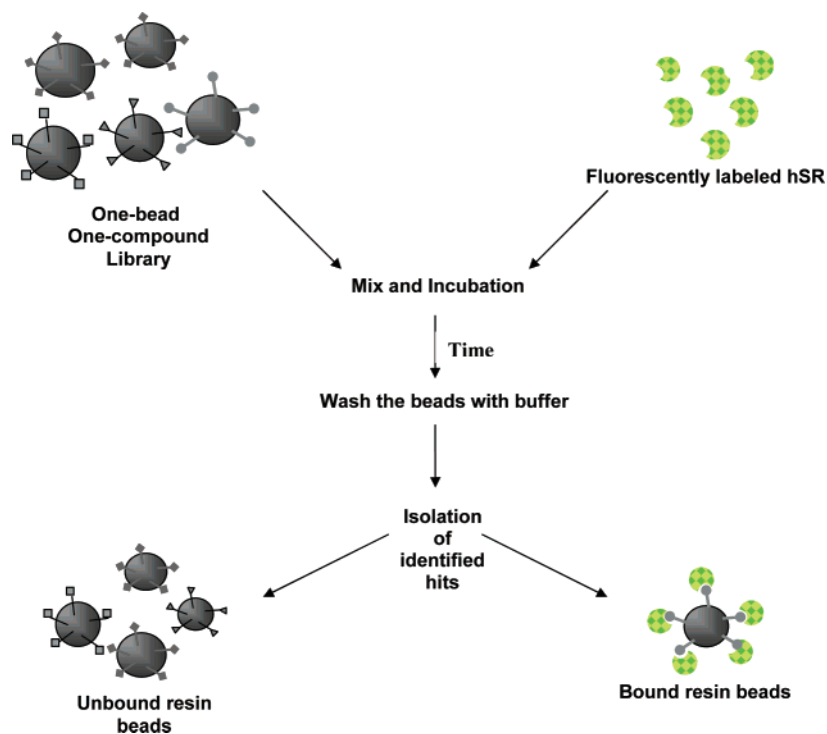
<sup>‡</sup> Department of Internal Medicine, UC Davis Cancer Center, University of California.

<sup>§</sup> Technion-Israel Institute of Technology.

<sup>a</sup> Abbreviations: hSR, human serine racemase; PLP, pyridoxal 5'-phosphate, TEA, triethanolamine; DAAO, D-amino acid oxidase; LDH, lactate dehydrogenase; DTT, dithiothreitol, ATP, adenosine triphosphate, NADH, reduced nicotinamide adenine dinucleotide.



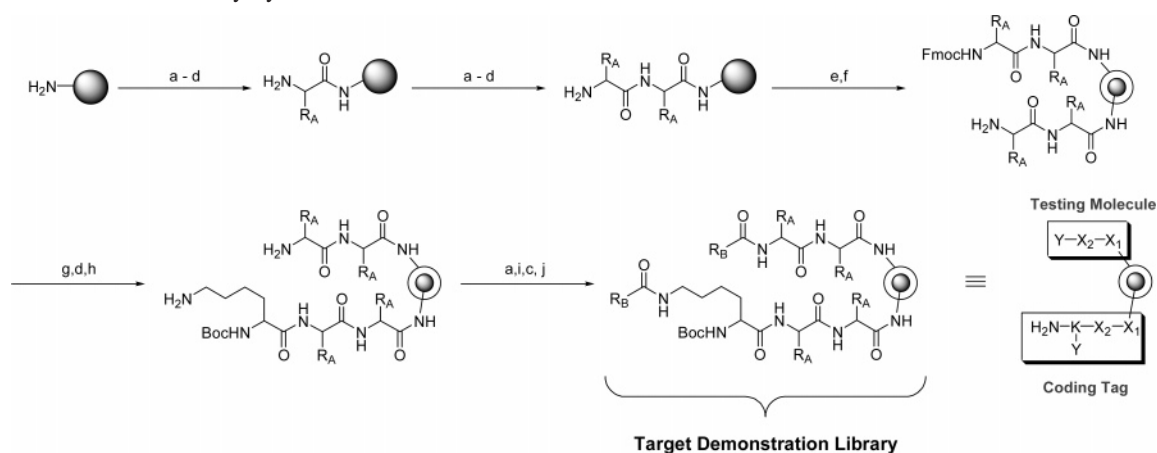
**Figure 1.** The involvement of hSR and D-serine in NMDA receptor activation. Glutamate stimulates the release of D-serine which works in concert with L-glutamate at the NMDA receptor.



**Figure 2.** Schematic of the bead library screening procedure employed.

employed in the synthesis are presented in the Supporting Information. Tentagel resin was employed because of its ability to swell appreciably in organic and aqueous solvents as well as its ability to tolerate acidic and basic reaction conditions without cleavage of the target molecule or the encoding tags. Auto-fluorescence of resin bound libraries, which has plagued

previous on-bead fluorescence-based assays, was observed in this model library. However, the previously observed inherent fluorescence of the Tentagel beads was not the origin of this auto-fluorescence.<sup>39</sup> Rather, certain combinations of diversity elements produced distinct auto-fluorescence in the absence of labeled hSR. This problem was addressed by measuring the

**Scheme 1.** Demonstration Library Synthesis<sup>a</sup>

<sup>a</sup> Reagents and conditions: (a) Split resin beads; (b) 42 Fmoc-amino acids (FmocNH-CH(R<sub>A</sub>)-OH), HOBT/DIC, DMF; (c) mix resin beads; (d) 25% piperidine in DMF; (e) H<sub>2</sub>O, 48 h; (f) Fmoc-Osu, DIEA, DCM/Et<sub>2</sub>O; (g) Boc-Lys(Dde)-OH, HOBT/DIC, DMF; (h) 2% hydrazine in DMF; (i) 42 carboxylic acids (R<sub>B</sub>-CO<sub>2</sub>H), HOBT/DIC, DMF; (j) TFA, TIS, phenol, EDT, H<sub>2</sub>O.

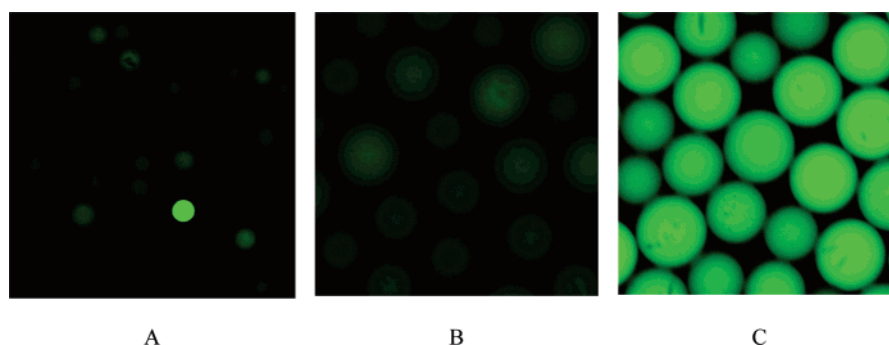
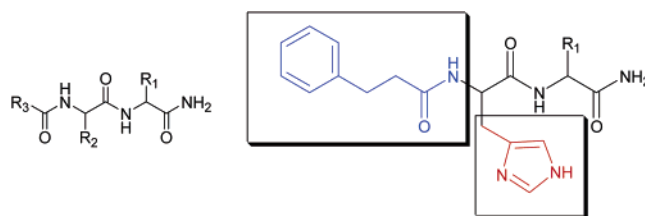


**Figure 3.** (A) Example of a positive bead in a background of negative ones. (B) Beads containing ligand **11** incubated in the absence of labeled hSR. (C) Beads containing ligand **11** incubated with AlexaFluor 488 labeled hSR.

auto-fluorescence intensity of the library through three emission filters (UV band-pass 360/40, FITC band-pass 490/20, and Texas Red band-pass 570/20). The percentages of auto-fluorescing beads found with these filters were: UV = 2%, FITC = 0.1%, and Texas Red = 0.5%. On the basis of these results, a protein dye having emission in the green region of the fluorescent spectra (Alexa Fluor 488) was selected.

Alexa Fluor 488 succinimidyl ester, which is specific for modification of the  $\epsilon$ -amino group of lysine residues, was used to modify hSR. The average dye:protein ratio obtained was 1.3:1, and the activity of hSR was not significantly affected by this labeling; on average, 93% of the original activity was retained after labeling and column purification. A thiol reactive dye (Alexa Fluor 488 C<sub>5</sub> maleimide) was also tested, but this dye caused an activity loss of >90% under similar conditions and was, therefore, not employed.

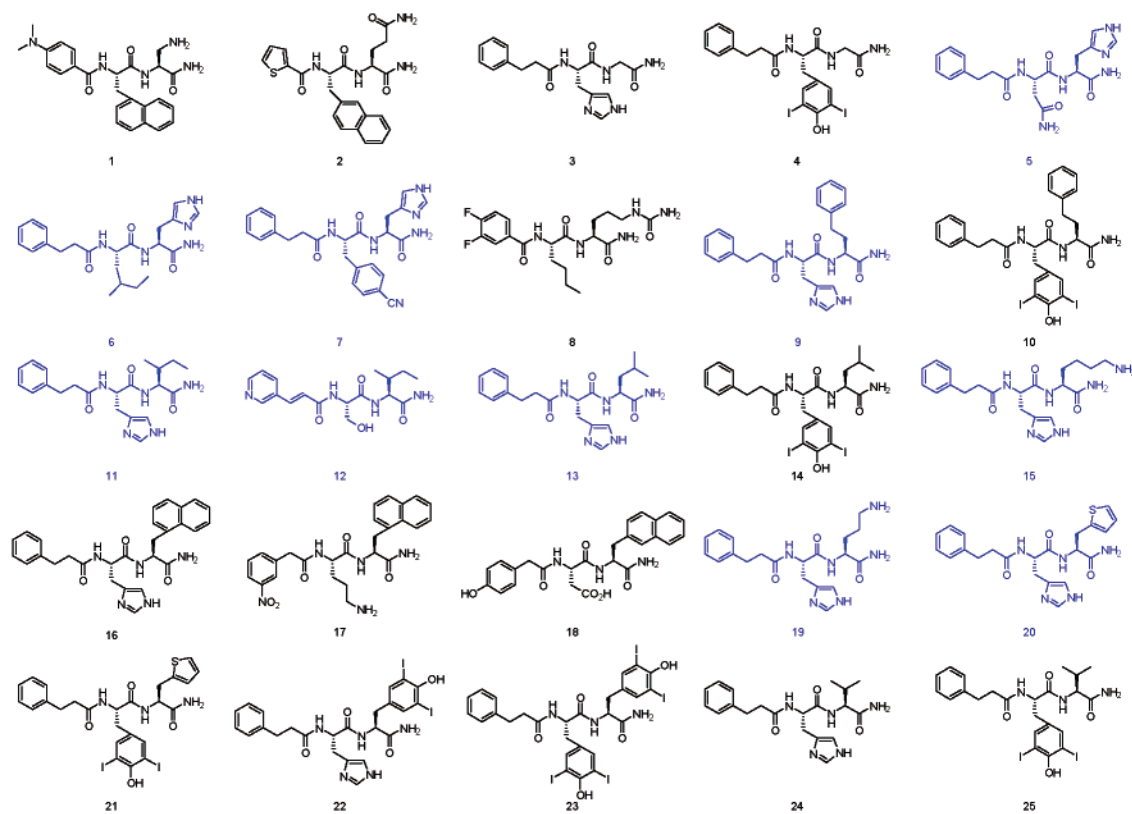
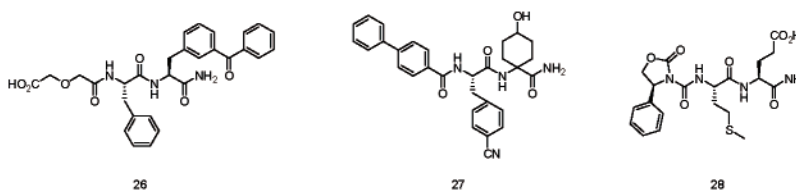
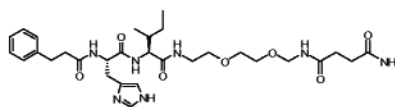
After incubation with the labeled hSR the beads were washed with buffer lacking hSR and then observed under the microscope. The brightest green fluorescent beads (Figure 3A) were isolated manually; sixty positive and three negative beads (for controls) were isolated from the ~75 000 (three 25 000-bead samples) beads screened. While these three cross-sections of beads would clearly not encompass the entire library, it was decided that screening these three bead cross-sections would represent a significant number of the compounds in the library.<sup>43</sup> Twenty-five of the positive beads were randomly selected and the three negative beads were washed with 8 M guanidine and then water to remove hSR from the bead surface, and the coding tags were sequenced by Edman degradation to determine the structures of the test compounds on the surface of the beads.



**Figure 4.** The overall structural of the peptide library with points of diversity denoted by R<sub>n</sub>. The observed structural motif in the inhibitors contains the 3-phenylpropionic acid moiety (blue) and the histidine moiety (red).

As a test, the screening method was further validated by resynthesizing ligand **11** (picked randomly from the identified hits) on Tentagel resin. These single compound beads did not fluoresce in the absence of labeled hSR (Figure 3B). However, when they were incubated with the labeled hSR, all were strongly positive (Figure 3C). After this test, the remaining sequences were resynthesized on Rink amide resin and liberated to yield amidated peptide products, and purified by HPLC to 95–99% purity. Clear structural motifs were found in the 25 identified peptides: 19 (76%) incorporated the 3-phenylpropionic acid moiety and 10 (40%) incorporated a histidine (Figure 4). Note also that 6 (24%) of the identified peptides incorporated a diiodo-tyrosine moiety, although the significance of this is unclear since these compounds were too insoluble to study. It remains possible that these are false positives.

The structures studied in inhibition assays (performed in the presence of 2 mM inhibitor) are summarized in Figure 5. Of the 25 compounds identified from positive beads, 10 of the

Identified HitsNegative ControlsDerivatization

29

**Figure 5.** Structures of binding and negative control compounds identified in hSR screen. Blue structures represent compounds that had sufficient solubility for inhibition studies and black structures depict structures that were not sufficiently soluble. Also included is a depiction of linker-derivatized structure **11**.

peptides were sufficiently soluble in the assay to allow their kinetic analysis (blue structures in Figure 5). The effects of these compounds on the activity of hSR are summarized in Table 1. The black figures depicted in Figure 5 were not fittingly soluble for inhibition studies. Control experiments in which D-serine was added to the assays instead of L-serine demonstrated that the lowered activity was not due to inhibition of the coupling enzymes. The two most potent inhibitors, **9** and **11**, were subjected to full inhibition analysis (Figure 6). The data fit best, as shown, to a model in which the inhibitors are competitive with respect to L-serine. The  $K_I$  values for **9** and **11** obtained

from global fitting of inhibition data sets to eq 1 are  $320 \pm 70 \mu\text{M}$  and  $610 \pm 120 \mu\text{M}$ , respectively.

After incubation of the bead library with labeled enzyme solution, the beads were washed with buffer lacking enzyme. Therefore, only compounds that slowly dissociate from hSR are expected to be identified. Figure 7 shows the time dependence for the inhibition of hSR by the four strongest inhibitors. The significant decrease in activity upon initial mixing of the inhibitors with hSR provides support for the inhibition model presented in Figure 8. The decrease in enzyme activity over  $\sim 30$  min clearly shows the slow binding character of these

**Table 1.** Inhibition of hSR by Resynthesized Hits Identified in the Fluorescent Enzyme Based Screen

compound <sup>a</sup>	percent decrease in hSR activity
5	42 ± 4
6	54 ± 2
7	72 ± 3
9	70 ± 3
11	74 ± 9
12	10 ± 1
13	57 ± 2
15	40 ± 2
19	49 ± 14
20	68 ± 6
26	4 ± 3
27	0
28	8 ± 2
29	0

<sup>a</sup> Compounds were tested at 2 mM.

inhibitors. Figure 9 presents data demonstrating the slow dissociation of **9** from hSR, which occurs with a half-life of ~3 min under these conditions.

Three nonfluorescent beads were picked as negative controls. The structures of the peptides on these beads are given in Figure 5. They show no obvious structural resemblance to those from the positive beads, and they do not significantly inhibit hSR. Also, these negative controls produce no hSR activity loss nor are they simply very slowly binding hSR ligands (i.e., they maintain a linear curve over time during the kinetic assays). Since histidine and phenylpropionic acid are important components of the structural motif, they were also tested as inhibitors at 2 mM in the hSR activity assay. No inhibition was observed with these compounds. To simulate a more beadlike environment and increase water solubility, inhibitor **11** was further derivatized with a linker to give **29** (Figure 5). The introduction of this linker did not improve inhibition, and was, in fact, detrimental to it; water solubility, however, was increased slightly. No

further attempts to derivatize ligands were made in light of the detrimental effect of the solubilizing linker on the ability of **11** to inhibit hSR.

## Discussion

The overproduction of glutamate has been implicated in a large number of acute and chronic degenerative conditions, including stroke, epilepsy, peripheral neuropathies, and chronic pain as well as Parkinson's, and Alzheimer's and Huntington's disease.<sup>9,44–46</sup> During stroke and other degenerative conditions, excessive glutamate is released, which is toxic to neurons. The harmful effects of excessive glutamate are believed to occur mainly through activation of the NMDA subtype of glutamate receptor.<sup>47</sup>

NMDA receptors have two sites that must be occupied for calcium influx through the receptor to take place.<sup>47</sup> Previously it was thought that glycine, in combination with L-glutamate, was the required ligand for the second site; however, it was recently demonstrated that D-serine is the principal activator of this site.<sup>48</sup> The involvement of D-serine in NMDA receptor activation apparently provides a failsafe mechanism to prevent over-activation of NMDA receptors by L-glutamate, which is abundant in the body. Inhibitors of hSR could therefore potentially be used as treatments for several neurodegenerative diseases, since they would provide a novel way to block the harmful effects of glutamate over-stimulation.

While the X-ray structure of hSR is not presently available, its amino acid sequence is homologous (40% identity) to that of *E. coli* catabolic threonine dehydratase whose structure has been determined.<sup>49,50</sup> A homology model of hSR based on catabolic threonine dehydratase was not considered of sufficient quality to be used as a basis for structure-based drug design due to the relatively low homology between the sequences. Therefore, we turned to combinatorial chemistry for the discovery of non-substrate-like, active site-directed inhibitors.

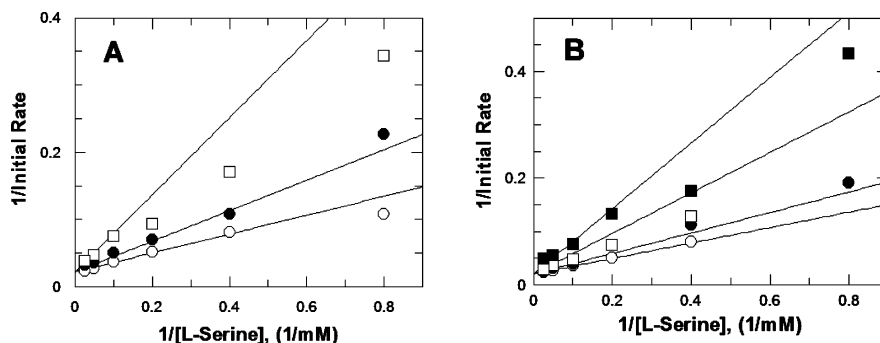


**Figure 6.** Double-reciprocal plot for inhibition of hSR by **9** and **11**. (A) The concentrations of **9** are 0 (◇), 0.2 (◆), and 1 (□) mM. (B) The concentration of **11** are 0 (◇), 0.2 (◆), 1 (□), and 2 (■) mM. The lines are those predicted from global fitting of the data sets to eq 1. A 40 min preincubation with inhibitors was employed. The  $K_i$  values obtained from these data are: **9**,  $320 \pm 70 \mu\text{M}$ ; **11**,  $610 \pm 120 \mu\text{M}$ .

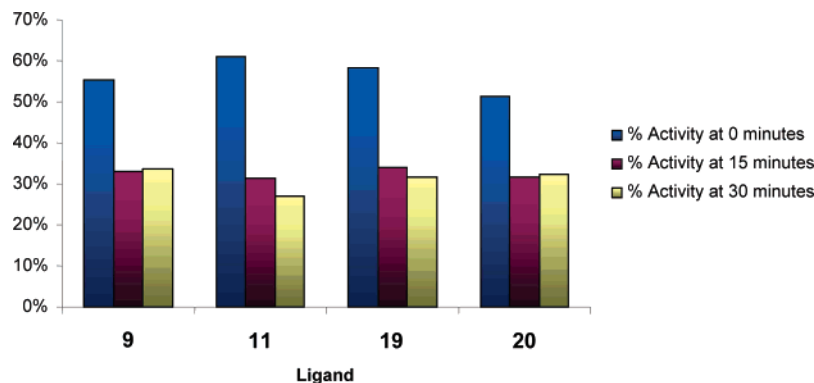


**Figure 7.** Percent activity of hSR vs incubation time with 2 mM of the indicated ligands.



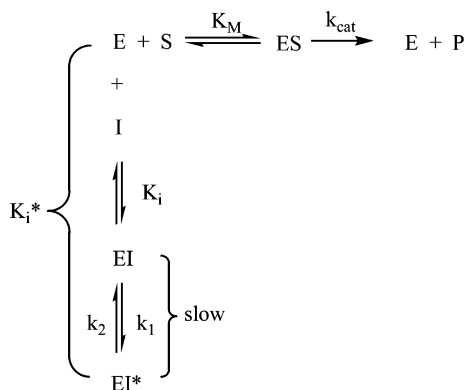


**Figure 8.** Mechanism of slow binding competitive inhibition.

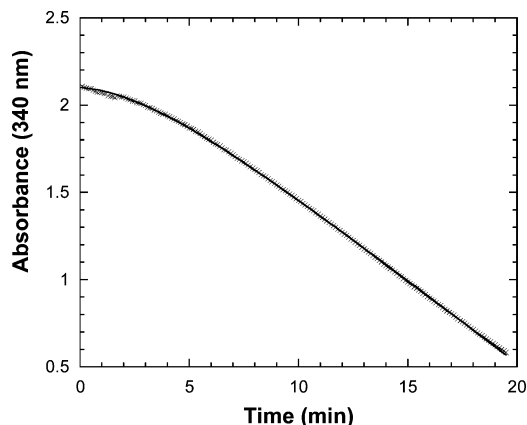


**Figure 9.** Slow dissociation of **9** from its complex with hSR. The hSR–inhibitor complex was diluted into a reaction mixture lacking inhibitor and containing 100 mM L-serine and the inhibitor dissociation half-life was measured. Here, the absorbance is that of NADH at 340 nm.

The application of combinatorial chemistry to biological ligand discovery has increased dramatically over the past decade,<sup>28,51–53</sup> and many examples exist in the literature of the discovery of both peptidic and nonpeptidic ligands of biological molecules with this methodology.<sup>28,51</sup> The size of the compound library explored in a given experiment is largely limited by the nature of the screening process. The large-scale screening of individual compounds, for example, is labor and materials intensive. The one-bead one-compound approach can deliver large libraries (100 000 to 1 000 000 compounds) rapidly, and these beads can be screened efficiently, in parallel, by high-throughput methods.<sup>31, 54</sup>

The application of on-bead assays provides the required high-throughput character of the screen, and recent studies show quantitative correlation between the results of on-bead and solution phase screening of identical libraries.<sup>53</sup> On-bead assays have the additional requirement that the test compound on the surface be identified from a single bead. This has been achieved in some cases by direct mass spectrometric analysis of test compounds cleaved from the resin.<sup>55</sup> More generally, encoding tags have been employed.<sup>42</sup> The advent of topologically segregated beads with test compounds presented on the surface and encoding tags in the interior of the beads has greatly facilitated on-bead discovery.<sup>42</sup>

Given these developments, we screened for hSR inhibitors via on-bead assay of one-bead one-compound combinatorial libraries in which the coding tags were topologically segregated from the test compounds on the bead surface. Figure 3A demonstrates the excellent signal-to-noise ratio obtained by direct binding of fluorescently labeled hSR to the bead library

followed by washing in enzyme-free solution. The strong signal observed suggests that automation using bead sorting instruments<sup>56</sup> can be employed with hSR in the future.

The on-bead assay procedure employed here includes a step where the beads are washed with hSR-free buffer after the initial 60 min binding incubation. This washing step brings about a thermodynamic driving force for hSR dissociation from the beads since the free/bound equilibrium is perturbed. We expected this procedure to select for tight binding inhibitors and were surprised to find the high micromolar inhibition constants for the best inhibitors (**9** and **11**). For example, if the inhibitors were to bind via a simple one-step mechanism, association rate constants of  $10^6$ – $10^8$   $M^{-1} s^{-1}$  would be expected. To get dissociation half-lives on the order of 10 min (as required to observe positive beads by fluorescence microscopy), this requires that the  $K_i$  values be  $10^{-9}$ – $10^{-11}$  M. Clearly, an alternative binding mechanism must be operative.

The existence of slow-binding enzyme inhibitors is well precedented in the literature.<sup>57</sup> The slow binding mechanism presented in Figure 8 can readily account for our observed results. The inhibitor initially binds in a loose complex with the enzyme, followed by slow isomerization to the final tighter complex. The key feature for the present discussion is the slow nature of the isomerization step, which would come to equilibrium during the preincubation with enzyme. The data presented in Figure 7 strongly supports the hypothesis that all of inhibitors discovered here follow the slow-binding mechanism of Figure 8 since there is an initial rapid decrease in activity followed by slower loss of activity. The data presented in Figure 9 for **9** provides additional and unequivocal evidence that this inhibitor slowly dissociates from the hSR–**9** complex. Remarkably, we have selectively isolated slow-binding hSR inhibitors simply by washing the beads free of excess hSR before fluorescent bead isolation.

The absence of a second class of inhibitors (i.e., tight binding) in this work implies they are not present in this relatively small library. In an attempt to identify tight binding inhibitors, we performed an experiment in which the labeled enzyme was further diluted (0.22 nM) and not removed prior to the screening process. The structures identified in this experiment are given in the Supporting Information. The ligands proved not to be inhibitors after resynthesis and inhibition assay. This suggests that the isolated beads were auto-fluorescing false-positives, which is consistent with the observed decrease in fluorescent bead frequency as a function of enzyme concentration (data not shown) and the frequency of auto-fluorescing beads observed in the absence of enzyme. Pre-sorting the beads with an automated bead sorter (which was not available at the time of this work) would eliminate false positive beads from the library before screening, which might allow the identification of rare tight binding inhibitors that might possibly be present.

The fact that ligands with millimolar  $K_D$  values are readily identified in assays that include only nanomolar concentrations of enzymes gives the experimentalist pause. One calculates the average concentration of ligands throughout the volume of the Tentagel beads used here to be 0.31 M. The structure of the Tentagel polystyrene-PEG copolymer is expected to be uniform throughout the volume of the bead since it is a 1% cross-linked polystyrene matrix modified heavily (50–70% w/w) with PEG. The termini of the latter contain the amino functional group onto which the peptides are connected. Therefore, it is reasonable to assume that the concentration of the test molecules is constant throughout the outer layer of the beads. This has significant ramifications for enzyme binding.

One would like to know the extent to which enzyme within the accessible bead volume is bound to PEG-attached test ligand. The present experimental situation is conceptually analogous to equilibrium dialysis experiments commonly used in biochemistry to measure the  $K_D$  for ligand binding to macromolecules. In equilibrium dialysis, the protein is contained within a dialysis membrane; itself immersed in a much larger volume of ligand-containing buffer. The small molecule ligand is free to diffuse in and out of the protein-containing dialysis container membrane and a binding equilibrium between protein and ligand is established. Here, the test ligand is constrained to be within the volume of the bead by the covalent tether to PEG. As an approximation, the present experimental situation is therefore treated as a equilibrium dialysis experiment in order to calculate the extent of enzyme binding to the test ligands during the period of incubation of enzyme with beads (i.e., before the beads are washed with enzyme-free buffer).

The  $K_D$  values found for the inhibitors here are  $\sim 1$  mM, while the hSR concentration in the experiment was 3.6 nM. Using these values and an on-bead ligand concentration of 0.3 M, one calculates that the hSR found within the bead volume is 99.6% bound to test ligand, resulting in strong accumulation of enzyme within the accessible bead volume and a consequent strong fluorescence signal. This is due to the concentration ( $\sim 0.3$  M) of the test ligand in the accessible bead volume being much greater than the  $K_D$  value ( $\sim 1$  mM) for the ligand, thermodynamically driving the binding of the relatively low affinity ligand to the low concentration of enzyme.

The volume of the bead that is accessible to the enzyme is likely to be a very small fraction of the total bead volume. This can be inferred from the present experimental results, which showed that with 4 mL of 3.6 nM enzyme (14 pmol)  $\sim 50$  beads were strongly fluorescent. If the complete bead volume were enzyme-accessible, then the  $\sim 150$  pmol of test ligand from the single tightest binding bead would bind the majority of the enzyme present in the experiment. The fact that a much larger number of beads were observed to be strongly fluorescent, and a variation in the affinity of the test ligands on these beads was found strongly suggests that only a thin layer of the surface is enzyme accessible. This latter conclusion is supported by the following simple calculations. The number of test ligands in the outer layer of a bead (one enzyme thickness;  $\sim 50$  Å at its narrowest) is  $5.0 \times 10^{10}$ , which when projected onto the bead surface gives  $9.4 \times 10^{17}$  test ligands/m<sup>2</sup>. A close-packed enzyme monolayer gives  $\sim 5.1 \times 10^{16}$  enzymes/m<sup>2</sup>, or  $\sim 18$  test ligands in the area occupied by one enzyme. Apparently, the polymer/ligand density would preclude significant enzyme penetration into the bead and the observed fluorescence is due to surface-bound enzyme. This also agrees with the reported size-exclusion limit of  $\sim 14$  kD for 1% cross-linked polystyrene,<sup>58</sup> the basis for Tentagel, and the hSR dimer molecular weight of 74 kD.<sup>59</sup> Restriction of enzyme binding to the surface layer explains the large number of observed fluorescent beads since only  $\sim 0.08$  pmol of test ligand/bead are present in this layer, which is small compared to the 14 pmol of enzyme present.

The high ligand concentration on the bead surface allows beads with low affinity ligands to bind sufficient enzyme to be detected by fluorescence in the present experiments. These beads with low affinity ligands and the auto-fluorescing beads create a background against which it is difficult to detect selectively beads with high affinity ligands, which are by nature more rare. The auto-fluorescing beads can, in principle, be removed by automated pre-sorting of the library. The problem posed by the beads with low affinity ligands can be addressed in either of

two ways. The first is to lower the concentration of the test ligands on the bead surface by partially capping the amino functional groups on the outer layer. This has recently been applied successfully<sup>16,60</sup> but as a general protocol is likely to result in significantly lower detection sensitivity due to the lower density of protein bound to the surface containing fewer ligands. A more general protocol that does not, in principle, lower the sensitivity for detecting hit beads is to include a soluble competitive inhibitor in the enzyme-containing binding buffer. The inhibitor concentration can be adjusted to fine-tune the desired selectivity for ligand affinity. In the present case, for example, the inclusion of 100 mM of an inhibitor with 0.1 mM  $K_D$  would be sufficient to prevent in large part beads with 1 mM  $K_D$  ligands from binding enzyme, with only beads having  $K_D$  values lower than this being readily detected. One can also envision a "boot-strap" procedure in which broad primary libraries are synthesized and screened to find low millimolar inhibitors, followed by synthesis of more focused secondary libraries based on motifs from the primary library, which are screened in the presence of the initial millimolar hit(s) as a competitive inhibitor to increase sensitivity for higher affinity ligands.

Importantly, the results presented here show that non-substrate-like inhibitors of hSR can indeed be readily discovered. Even though these inhibitors are structurally unrelated to the natural substrate serine, they are in fact competitive with it indicating they bind at the same site (i.e., the active site). This is an important result since the design of inhibitors based on the natural substrate serine is likely to incur nonspecificity problems since a very large number of enzymes utilize this common amino acid. Inhibitors that are structurally unrelated to the natural substrate will have a much greater chance of being specific for hSR. While it is true that the structural motif observed in the identified inhibitors (i.e., the carbon backbone of phenylalanine and the imidazole ring) is unrelated to serine, phenylalanine, and histidine are quite common in cells. Importantly, the present results show that the active site does have the ability to accommodate large functional groups (e.g., phenyl and imidazole rings) which provides an excellent opportunity to design libraries of highly diverse inhibitors that are not limited to the hydroxymethyl group of serine.

## Experimental Section

**Peptide Library Synthesis.** The synthesis of the encoded, peptide library was initiated by swelling the Tentagel beads (2.0 g, 130  $\mu$ m; capacity: 0.32 mmol/g) in a 50 mL plastic column in DMF for 120 min. The DMF was drained and the beads were distributed equally into 42 plastic columns (1 mL) that were secured in a Teflon block. One of the amino acid diversity elements (3 equiv), as well as HOBt (3.5 equiv) and DIC (3.5 equiv), was added to each column. The Teflon block was placed on a shaker and reactions were allowed to proceed for 2 h. After Kaiser tests were negative for each column, the beads were washed ( $5 \times$  DMF,  $5 \times$  MeOH,  $5 \times$  DCM,  $5 \times$  DMF) in an appropriate volume based on plastic column size and pooled. Next, 25% piperidine in DMF was added and the columns were rotated for 5 min. The liquid was drained and a fresh solution of 25% piperidine/DMF was added and the column was rotated for another 15 min. Once the Fmoc deprotection was complete, the resin was redistributed and the procedure repeated. When the second amino acid had been added and the Fmoc group removed, the beads were pooled, dried thoroughly, and then swollen in water for 48 h, after which Fmoc-Osu (0.5 equiv) dissolved in ether/DCM (55:45) and DIEA was added (2 equiv). The column was shaken vigorously for 30 min, after which the solution was drained. The beads were washed and Boc-Lys(Fmoc) [3 equiv] was added, as well as HOBt (3.5 equiv)

and DIC (3.5 equiv). The column was rotated for 2 h, after which a Kaiser test was negative. The beads were then redistributed to the 42 columns, secured in the Teflon block, and to each column was added one of the carboxylic acid diversity elements (10 equiv) as well as HOBt (13 equiv) and DIC (13 equiv). When the Kaiser test was negative for all columns, the beads were pooled and the deprotection of all the remaining protecting groups was performed with an appropriate volume of 82.5% TFA, 5% phenol, 5% thioanisole, 5% H<sub>2</sub>O, and 2.5% TIS and rotation for 2 h. After the final deprotection, the beads were neutralized with DIEA in DMF and then washed thoroughly with: DMF (8 × 5 mL), 20% H<sub>2</sub>O/DMF (8 × 5 mL), 40% H<sub>2</sub>O/DMF (8 × 5 mL), 60% H<sub>2</sub>O/DMF (8 × 5 mL), 80% H<sub>2</sub>O/DMF (8 × 5 mL), H<sub>2</sub>O (8 × 5 mL), MeOH (8 × 5 mL), DCM (8 × 5 mL), dried in a vacuum desiccator, and stored in distilled water containing 0.1% NaN<sub>3</sub>.

**Enzyme Preparation.** The hSR gene was PCR amplified with primers that encoded NdeI/BamHI restriction sites, allowing in-frame cloning into pET28a. BL21-CondonPlus(DE3)-RIL cells containing pET28a-hSR were grown at 37 °C in LB medium to an OD<sub>600</sub> ≈ 0.5. The temperature was lowered to 25 °C, cells were grown to OD<sub>600</sub> ≈ 0.8, induced with 0.5 mM IPTG, and grown for 16 h in an 8 L media at 25 °C. Cells were harvested by centrifugation and the paste was resuspended in buffer A (50 mM TEA·HCl, 150 mM KCl, 50 μM PLP, pH 8.0) with 10 mM imidazole. Cells were disrupted by sonication, and the homogenate was clarified by centrifugation. Soluble extract was loaded on a 8 mL column of Ni-NTA resin. After washing the column with buffer A plus 20 mM imidazole, the column was eluted with a linear 20–300 mM imidazole gradient in buffer A. Fractions were assayed for activity and analyzed by SDS-PAGE. Fractions containing pure hSR were pooled, concentrated, flash-frozen, and stored at –80 °C in Ni-column starting buffer.

**hSR Activity Assay.** The initial rate of the combined racemization and elimination reactions catalyzed by hSR was followed by coupling to lactic dehydrogenase (LDH). D-Serine derived from L-serine was oxidized with D-amino acid oxidase (DAAO) to give β-hydroxy pyruvate, while the elimination reaction produces pyruvate directly. Total activity of racemic β elimination was monitored by the decrease in NADH absorbance at 340 nm. Reaction mixtures for the activity assay contained 200 mM TEA·HCl, 150 mM KCl, 50 μM PLP, 5 mM MgCl<sub>2</sub>, 2 unit/mL DAAO, 10 unit/mL LDH, 10 mM DTT, 2.5 mM ATP, 0.3 mM NADH and varying concentrations of L-serine.

**Protein Labeling.** Dye labeling was performed according to the manufacturer's instructions. All protein labeling and bead screening procedures were protected from light. The labeling reaction consisted of 100 μL of 1.44 mg/mL hSR in buffer A containing 0.1 mM PLP, 0.5 mM MgCl<sub>2</sub>, 0.5 mM CaCl<sub>2</sub>, and 0.02 mg Alexa Fluor 488 succinimidyl ester for 45 min with stirring. The activity of the enzyme was monitored as a function of reaction time. The reaction was terminated and the enzyme purified from excess dye by passing the reaction solution over a Sephadex G-25 spin column equilibrated with buffer A.

**Library Pre-screening, Screen, and Isolation of Hits.** Three samples of the Tentagel beads (approximately 75 000) containing the peptide library X<sub>2</sub>-Acid<sub>1</sub> were swollen in 1 mL buffer B (120 mM TEA·HCl, [pH 8.0], 137 mM NaCl, 27 mM KCl, 0.2% Tween-20, 0.1% gelatin, 0.05% NaN<sub>3</sub>) for 60 min. The enzyme solution used for bead screening contained 3.6 nM Alexa Fluor 488 labeled hSR in buffer B. The beads were then incubated with 1 mL of labeled hSR for 60 min at room temperature, after which the beads were washed with 1 mL of Buffer B six times. The beads were visualized under a fluorescence microscope fitted with a long-band green filter. The brightest beads were isolated manually with a pipet tip.

**Edman Degradation Sequencing.** The isolated beads were washed three times with 8 M guanidine-HCl for 1 min each and three times with water. The sequencing of the encoding peptide tags was performed on an ABI 494 Protein Sequencer using a modified program and gradients described in the literature.<sup>61</sup>

**Resynthesis and Characterization of Peptides.** Larger-scale synthesis of the peptides identified as hSR binders was performed on 150 mg of Fmoc-Rink MHBA amide resin (capacity: 0.65 mmol/g). The beads were swollen in DMF for 60 min, drained and then treated with 3 mL of 25% piperidine in DMF twice; first for 5 min, next for 15 min. After Fmoc deprotection, the beads were washed with DMF (5 × 3 mL) and the peptide sequence was constructed using the appropriate amino (3 equiv) and carboxylic (10 equiv) acids along with HOBt and DIC (3.5 equiv each and 13 equiv respectively). The peptide was cleaved from the resin using 3 mL 95% TFA, 2.5% H<sub>2</sub>O, and 2.5% TIS for 2 h. The cleavage solution was collected and concentrated by evaporation, and 5–10 mL of ether was added until the product had completely precipitated. The filtrate was cooled to –80 °C for 14 h and centrifuged. The precipitated product was dried under vacuum for 24 h. The dried product was then purified by HPLC, collected fractions were lyophilized, and the resulting solids were subjected to HPLC and ES-MS analysis. See Supporting Information for details.

**Inhibition Curve Fitting.** The initial rate of hSR in the presence of peptide inhibitors was measured with varying concentrations of L-serine and several fixed concentrations of the peptide. The reaction mixture was incubated with inhibitor for 40 min prior to being initiated by addition of L-serine. The value of K<sub>I</sub> was determined by curve fitting to eq 1, where *v* is the initial rate, V<sub>max</sub> is the maximal velocity, K<sub>M</sub> the Michaelis constant, I the hSR inhibitor, and K<sub>I</sub> the inhibition constant.

$$v = \frac{V_{\max} \cdot [S]}{K_m \left( 1 + \frac{[I]}{K_i} \right) + [S]} \quad (1)$$

**Measurement of Slow-Binding Association and Dissociation Half-Life.** Peptide **9** was chosen to measure the inhibitor dissociation half-life. hSR was incubated with 50 mM TEA·HCl pH 8.0, 50 μM PLP, and 2 mM **9** for 1 h. Two microliters of this preincubated hSR solution was mixed with 98 μL of 200 mM TEA·HCl (pH 8.4), 150 mM KCl, 50 μM PLP, 5 mM MgCl<sub>2</sub>, 2 unit/mL DAAO, 10 unit/mL LDH, 10 mM DTT, 2.5 mM ATP, 0.3 mM NADH and 100 mM L-serine, and the reaction was monitored at 340 nm. The ratio of the final inhibitor concentration to that of L-serine was very small, ensuring irreversible dissociation of inhibitor. The progress curves were fitted to eq 2.

$$A_{340} = A_{340}^0 + \left[ v_f t + \frac{(v_i - v_f)(1 - e^{-kt})}{k} \right] \quad (2)$$

Here, A<sub>340</sub> is the NADH absorbance at 340 nm, *v*<sub>i</sub> the initial reaction rate, *v*<sub>f</sub> the final reaction rate, and *k* the apparent dissociation rate constant. Figure 8 shows the mechanism for slow binding where an initial encounter complex with inhibitor isomerizes to give the final complex.

**Acknowledgment.** We thank Dr. Michael Paddy and Dr. Richard Harris for their help and training on the microscopes. We also thank Lori Robins, Melissa Jeddelloh, and Sung Hee Hwang for helpful discussions. Finally we would like to thank Dr. Michael Nantz and Hasan Palandoken for the gracious use of their HPLC system. We thank the National Science Foundation CHE-0313888 for support of this work.

**Supporting Information Available:** Instrumentation, diversity elements, compound structures, mass spectral data, purity data, and analytical HPLC traces for target compounds. This material is available free of charge via the Internet at <http://pubs.acs.org>.

## References

- Miller, R. F. D-Serine as a glial modulator of nerve cells. *Glia* **2004**, 47 (3), 275–83.



- (2) Strisovsky, K.; Jiraskova, J.; Barinka, C.; Majer, P.; Rojas, C.; Slusher, B. S.; Konvalinka, J. Mouse brain serine racemase catalyzes specific elimination of L-serine to pyruvate. *FEBS Lett* **2003**, *535* (1–3), 44–8.
- (3) Panizzutti, R.; De Miranda, J.; Ribeiro, C. S.; Engelender, S.; Wolosker, H. A new strategy to decrease N-methyl-D-aspartate (NMDA) receptor coactivation: inhibition of D-serine synthesis by converting serine racemase into an eliminase. *Proc. Natl. Acad. Sci. U.S.A.* **2001**, *98* (9), 5294–9.
- (4) Schell, M. J.; Molliver, M. E.; Snyder, S. H. D-serine, an endogenous synaptic modulator: localization to astrocytes and glutamate-stimulated release. *Proc. Natl. Acad. Sci. U.S.A.* **1995**, *92* (9), 3948–52.
- (5) Ribeiro, C. S.; Reis, M.; Panizzutti, R.; de Miranda, J.; Wolosker, H. Glial transport of the neuromodulator D-serine. *Brain Res.* **2002**, *929* (2), 202–9.
- (6) Schell, M. J.; Brady, R. O., Jr.; Molliver, M. E.; Snyder, S. H. D-serine as a neuromodulator: regional and developmental localizations in rat brain glia resemble NMDA receptors. *J. Neurosci.* **1997**, *17* (5), 1604–15.
- (7) Danysz, W.; Zajaczkowski, W.; Parsons, C. G. Modulation of learning processes by ionotropic glutamate receptor ligands. *Behav. Pharmacol.* **1995**, *6* (5 and 6), 455–474.
- (8) Heresco-Levy, U.; Javitt, D. C. The role of N-methyl-D-aspartate (NMDA) receptor-mediated neurotransmission in the pathophysiology and therapeutics of psychiatric syndromes. *Eur. Neuropsychopharmacol.* **1998**, *8* (2), 141–52.
- (9) Hashimoto, A.; Oka, T. Free D-aspartate and D-serine in the mammalian brain and periphery. *Prog. Neurobiol.* **1997**, *52* (4), 325–53.
- (10) Contestabile, A. Roles of NMDA receptor activity and nitric oxide production in brain development. *Brain Res. Rev.* **2000**, *32* (2–3), 476–509.
- (11) Stevens, E. R.; Esguerra, M.; Kim, P. M.; Newman, E. A.; Snyder, S. H.; Zahs, K. R.; Miller, R. F. D-serine and serine racemase are present in the vertebrate retina and contribute to the physiological activation of NMDA receptors. *Proc. Natl. Acad. Sci. U.S.A.* **2003**, *100* (11), 6789–94.
- (12) Yang, Y.; Ge, W.; Chen, Y.; Zhang, Z.; Shen, W.; Wu, C.; Poo, M.; Duan, S. Contribution of astrocytes to hippocampal long-term potentiation through release of D-serine. *Proc. Natl. Acad. Sci. U.S.A.* **2003**, (100), 15194–9.
- (13) Wu, S.; Barger, S. W.; Sims, T. J., Schwann cell and epineurial fibroblast expression of serine racemase. *Brain Res.* **2004**, *1020*, (1–2), 161–6.
- (14) Uo, T.; Yoshimura, T.; Shimizu, S.; Esaki, N., Occurrence of pyridoxal 5'-phosphate-dependent serine racemase in silkworm, *Bombyx mori*. *Biochem Biophys Res Commun* **1998**, *246* (1), 31–4.
- (15) Foltyn, V. N.; Bendikov, I.; De Miranda, J.; Panizzutti, R.; Dumin, E.; Shleper, M.; Li, P.; Toney, M. D.; Kartvelishvili, E.; Wolosker, H., Serine racemase modulates intracellular D-serine levels through an alpha,beta-elimination activity. *J. Biol. Chem.* **2005**, *280* (3), 1754–63.
- (16) Swanson, R. A.; Ying, W.; Kauppinen, T. M. Astrocyte influences on ischemic neuronal death. *Curr. Mol. Med.* **2004**, *4* (2), 193–205.
- (17) Krystal, J. H.; D'Souza, D. C. D-serine and the therapeutic challenge posed by the N-methyl-D-aspartate antagonist model of schizophrenia. *Biol. Psychiatry* **1998**, *44* (11), 1075–6.
- (18) Hashimoto, K.; Fukushima, T.; Shimizu, E.; Komatsu, N.; Watanabe, H.; Shinoda, N.; Nakazato, M.; Kumakiri, C.; Okada, S.; Hasegawa, H.; Imai, K.; Iyo, M. Decreased serum levels of D-serine in patients with schizophrenia: evidence in support of the N-methyl-D-aspartate receptor hypofunction hypothesis of schizophrenia. *Arch. Gen. Psychiatry* **2003**, *60* (6), 572–6.
- (19) Hashimoto, K.; Fukushima, T.; Shimizu, E.; Okada, S.; Komatsu, N.; Okamura, N.; Koike, K.; Koizumi, H.; Kumakiri, C.; Imai, K.; Iyo, M. Possible role of D-serine in the pathophysiology of Alzheimer's disease. *Prog. Neuropsychopharmacol. Biol. Psychiatry* **2004**, *28* (2), 385–8.
- (20) Chen, Z.; Huang, W.; Srinivas, S. R.; Jones, C. R.; Ganapathy, V.; Prasad, P. D. Serine racemase and D-serine transport in human placenta and evidence for a transplacental gradient for D-serine in humans. *J. Soc. Gynecol. Investig.* **2004**, *11* (5), 294–303.
- (21) Wang, R.; Steensma, D. H.; Takaoka, Y.; Yun, J. W.; Kajimoto, T.; Wong, C. H., A search for pyrophosphate mimics for the development of substrates and inhibitors of glycosyltransferases. *Bioorg. Med. Chem.* **1997**, *5* (4), 661–72.
- (22) Compain, P.; Martin, O. R. Carbohydrate mimetics-based glycosyltransferase inhibitors. *Bioorg. Med. Chem.* **2001**, *9* (12), 3077–92.
- (23) Lee, L. V.; Mitchell, M. L.; Huang, S. J.; Fokin, V. V.; Sharpless, K. B.; Wong, C. H. A potent and highly selective inhibitor of human alpha-1,3-fucosyltransferase via click chemistry. *J. Am. Chem. Soc.* **2003**, *125* (32), 9588–9.
- (24) Hinou, H.; Sun, X. L.; Ito, Y. Systematic syntheses and inhibitory activities of bisubstrate-type inhibitors of sialyltransferases. *J. Org. Chem.* **2003**, *68* (14), 5602–13.
- (25) Alfaro-Lopez, J.; Yuan, W.; Phan, B. C.; Kamath, J.; Lou, Q.; Lam, K. S.; Hruby, V. J., Discovery of a novel series of potent and selective substrate-based inhibitors of p60c-src protein tyrosine kinase: conformational and topographical constraints in peptide design. *J. Med. Chem.* **1998**, *41* (13), 2252–60.
- (26) Al-Obeidi, F. A.; Lam, K. S., Development of inhibitors for protein tyrosine kinases. *Oncogene* **2000**, *19* (49), 5690–701.
- (27) Wennemers, H.; Conza, M.; Nold, M.; Krattiger, P., Diketopiperazine receptors: a novel class of highly selective receptors for binding small peptides. *Chemistry* **2001**, *7* (15), 3342–7.
- (28) Gibson, C.; Sulyok, G. A.; Hahn, D.; Goodman, S. L.; Holzemann, G.; Kessler, H., Nonpeptidic alpha(v)beta(3) Integrin Antagonist Libraries: On-Bead Screening and Mass Spectrometric Identification without Tagging. *Angew. Chem. Int. Ed. Engl.* **2001**, *40* (1), 165–169.
- (29) Opatz, T.; Liskamp, R. M. Synthesis and screening of libraries of synthetic tripodal receptor molecules with three different amino acid or peptide arms: identification of iron binders. *J. Comb. Chem.* **2002**, *4* (4), 275–84.
- (30) Thorpe, D. S.; Rosse, G.; Yeoman, H.; Wilson, S.; Willson, P.; Harlow, G.; Robinson, A.; Wertman, K. F. On-bead and solution screening approaches for genomically derived targets. Discovery of surrogate ligands and substrates using combinatorial chemistry libraries. *Methods Mol Biol* **2002**, *201*, 239–63.
- (31) Meldal, M. The one-bead two-compound assay for solid-phase screening of combinatorial libraries. *Biopolymers* **2002**, *66* (2), 93–100.
- (32) Groth, T.; Renil, M.; Meinjohanns, E. PEG based resins for protease drug discovery synthesis, screening and analysis of combinatorial on-bead libraries. *Comb. Chem. High Throughput Screen.* **2003**, *6* (7), 589–610.
- (33) Houghten, R. A.; Pinilla, C.; Blondelle, S. E.; Appel, J. R.; Dooley, C. T.; Cuervo, J. H. Generation and use of synthetic peptide combinatorial libraries for basic research and drug discovery. *Nature* **1991**, *354*, (6348), 84–6.
- (34) Lebl, M.; Krchnak, V.; Sepetov, N. F.; Seligmann, B.; Strop, P.; Felder, S.; Lam, K. S., One-bead-one-structure combinatorial libraries. *Biopolymers* **1995**, *37* (3), 177–98.
- (35) Lam, K. S.; Sroka, T.; Chen, M. L.; Zhao, Y.; Lou, Q.; Wu, J.; Zhao, Z. G. Application of "one-bead one-compound" combinatorial library methods in signal transduction research. *Life Sci.* **1998**, *62* (17–18), 1577–83.
- (36) Lam, K. S.; Liu, R.; Miyamoto, S.; Lehman, A. L.; Tuscano, J. M. Applications of one-bead one-compound combinatorial libraries and chemical microarrays in signal transduction research. *Acc. Chem. Res.* **2003**, *36* (6), 370–7.
- (37) Lam, K. S.; Lehman, A. L.; Song, A.; Doan, N.; Enstrom, A. M.; Maxwell, J.; Liu, R., Synthesis and screening of "one-bead one-compound" combinatorial peptide libraries. *Methods Enzymol.* **2003**, *369*, 298–322.
- (38) Hwang, S.; Tamilarasu, N.; Ryan, K.; Huq, I.; Richter, S.; Still, W. C.; Rana, T. M., Inhibition of gene expression in human cells through small molecule-RNA interactions. *Proc. Natl. Acad. Sci. U.S.A.* **1999**, *96* (23), 12997–3002.
- (39) Alluri, P. G.; Reddy, M. M.; Bachhawat-Sikder, K.; Olivos, H. J.; Kodadek, T., Isolation of protein ligands from large peptidic libraries. *J. Am. Chem. Soc.* **2003**, *125* (46), 13995–4004.
- (40) Hu, Y.; Helm, J. S.; Chen, L.; Ginsberg, C.; Gross, B.; Kraybill, B.; Tyanont, K.; Fang, X.; Wu, T.; Walker, S. Identification of selective inhibitors for the glycosyltransferase MurG via high-throughput screening. *Chem. Biol.* **2004**, *11* (5), 703–11.
- (41) Lam, K. S.; Lebl, M.; Krchnak, V., The "One-Bead-One-Compound" Combinatorial Library Methodology. *Chem. Rev.* **1997**, *97* (2), 411–448.
- (42) Liu, R.; Marik, J.; Lam, K. S., A novel peptide-based encoding system for "one-bead one-compound" peptidomimetic and small molecule combinatorial libraries. *J. Am. Chem. Soc.* **2002**, *124* (26), 7678–80.
- (43) Zhao, P.-L.; Zambias, R.; Bolonese, J.; Boultons, D.; Chapman, K., Sample size determination in combinatorial chemistry. *Proc. Natl. Acad. Sci. U.S.A.* **1995**, *92*, 10212–10216.
- (44) Krystal, J. H.; D'Souza, D. C.; Petrakis, I. L.; Belger, A.; Berman, R. M.; Charney, D. S.; Abi-Saab, W.; Madonick, S. NMDA agonists and antagonists as probes of glutamatergic dysfunction and pharmacotherapies in neuropsychiatric disorders. *Harv. Rev. Psychiatry* **1999**, *7* (3), 125–43.
- (45) Cull-Candy, S.; Brickley, S.; Farrant, M. NMDA receptor subunits: diversity, development and disease. *Curr. Opin. Neurobiol.* **2001**, *11* (3), 327–35.

- (46) Palmer, G. C.; Widzowski, D., Low affinity use-dependent NMDA receptor antagonists show promise for clinical development. *Amino Acids* **2000**, *19* (1), 151–5.
- (47) Nishizawa, Y., Glutamate release and neuronal damage in ischemia. *Life Sci.* **2001**, *69* (4), 369–81.
- (48) Mothet, J. P.; Parent, A. T.; Wolosker, H.; Brady, R. O., Jr.; Linden, D. J.; Ferris, C. D.; Rogawski, M. A.; Snyder, S. H., D-serine is an endogenous ligand for the glycine site of the N-methyl-D-aspartate receptor. *Proc. Natl. Acad. Sci. U.S.A.* **2000**, *97* (9), 4926–31.
- (49) Scarselli, M.; Padula, M. G.; Bernini, A.; Spiga, O.; Ciutti, A.; Leoncini, R.; Vannoni, D.; Marinello, E.; Niccolai, N., Structure and function correlations between the rat liver threonine deaminase and aminotransferases. *Biochim. Biophys. Acta* **2003**, *1645* (1), 40–8.
- (50) Gallagher, D. T.; Gilliland, G. L.; Xiao, G.; Zondlo, J.; Fisher, K. E.; Chinchilla, D.; Eisenstein, E., Structure and control of pyridoxal phosphate dependent allosteric threonine deaminase. *Structure* **1998**, *6* (4), 465–75.
- (51) Schmuck, C.; Heil, M., Using combinatorial methods to arrive at a quantitative structure–stability relationship for a new class of one-armed cationic peptide receptors targeting the C-terminus of the amyloid beta-peptide. *Org. Biomol. Chem.* **2003**, *1* (4), 633–6.
- (52) Yang, X.; Bassett, S. E.; Li, X.; Luxon, B. A.; Herzog, N. K.; Shope, R. E.; Aronson, J.; Prow, T. W.; Leary, J. F.; Kirby, R.; Ellington, A. D.; Gorenstein, D. G. Construction and selection of bead-bound combinatorial oligonucleoside phosphorothioate and phosphorodithioate aptamer libraries designed for rapid PCR-based sequencing. *Nucleic Acids Res.* **2002**, *30* (23), e132.
- (53) Smith, H. K.; Bradley, M. Comparison of resin and solution screening methodologies in combinatorial chemistry and the identification of a 100 nM inhibitor of trypanothione reductase. *J. Comb. Chem.* **1999**, *1* (4), 326–32.
- (54) Randell, K. D.; Barkley, A.; Arya, P., High-throughput chemistry toward complex carbohydrates and carbohydrate-like compounds. *Comb. Chem. High Throughput Screen.* **2002**, *5* (2), 179–93.
- (55) Wang, X.; Zhang, J.; Song, A.; Lebrilla, C. B.; Lam, K. S. Encoding method for OBOC small molecule libraries using a biphasic approach for ladder-synthesis of coding tags. *J. Am. Chem. Soc.* **2004**, *126* (18), 5740–9.
- (56) Yang, X.; Li, X.; Prow, T. W.; Reece, L. M.; Bassett, S. E.; Luxon, B. A.; Herzog, N. K.; Aronson, J.; Shope, R. E.; Leary, J. F.; Gorenstein, D. G. Immunofluorescence assay and flow-cytometry selection of bead-bound aptamers. *Nucleic Acids Res.* **2003**, *31* (10), e54.
- (57) Morrison, J. F.; Walsh, C. T. The behavior and significance of slow-binding enzyme inhibitors. *Adv. Enzymol. Relat. Areas Mol. Biol.* **1988**, *61*, 201–301.
- (58) Pittman, C. U.; Smith, L. R.; Hanes, R. M. Catalytic reactions using polymer-bound vs homogeneous complexes of nickel, rhodium, and ruthenium. *J. Am. Chem. Soc.* **1975**, *97* (7), 1742–8.
- (59) Hepner, F.; Pollak, A.; Ulfig, N.; Yae-Kyung, M.; Lubec, G. Mass spectrometrical analysis of human serine racemase in foetal brain. *J. Neural Transm.* **2005**, *112* (6), 805–11.
- (60) Wang, X.; Peng, L.; Liu, R.; Xu, B.; Lam, K. S. Applications of topologically segregated bilayer beads in 'one-bead one-compound' combinatorial libraries. *J. Pept. Res.* **2005**, *65* (1), 130–8.
- (61) Liu, R.; Lam, K. S. Automatic Edman microsequencing of peptides containing multiple unnatural amino acids. *Anal. Biochem.* **2001**, *295*, (1), 9–16.

JM050701C